

FaceME: Face-to-Machine Proximity Estimation Based on RSSI Difference for Mobile Industrial Human–Machine Interaction

Zhezhuang Xu¹, Member, IEEE, Rongkai Wang², Student Member, IEEE, Xi Yue, Ting Liu, Cailian Chen³, Member, IEEE, and Shih-Hau Fang⁴, Senior Member, IEEE

Abstract—In the mobile industrial human–machine interaction (HMI), to establish the data connection, the engineer has to manually select the target machine from a long list, which may lead to wrong connection and waste of time. We observe that the engineer should face to the machine during the interaction to ensure that the machine works accurately, and this characteristic makes the proximity estimation algorithm suitable to simplify the data connection. However, due to the densely deployed machines, the existing algorithms cannot provide sufficient accuracy with limited latency. In this paper, we implement a testbed to evaluate the performance in the mobile industrial HMI. Based on the experimental results, we propose the definition of received signal strength indicator (RSSI) difference and then use it to design the face-to-machine proximity estimation (FaceME) algorithm. The experimental results prove that FaceME can provide guaranteed estimation accuracy and low-time complexity.

Index Terms—Face-to-machine proximity, industrial Internet of things, industrial wireless sensor networks, mobile industrial human–machine interaction (HMI), proximity estimation, received signal strength indicator (RSSI) difference.

I. INTRODUCTION

WITH the evolution from industrial wireless sensor networks [1]–[4] to industrial Internet of things [5]–[7], considerable number of machines have been connected to the

Manuscript received January 3, 2018; revised March 21, 2018; accepted April 2, 2018. Date of publication April 24, 2018; date of current version August 1, 2018. This work was supported in part by the National Natural Science Foundation of China under Grant 61673116, Grant 61304260, Grant 61703106, Grant 61703105, Grant 61521063, Grant 61622307, and Grant U1405251 and in part by the Ministry of Science and Technology, Taiwan, under Grant MOST 107-2634-F-155-001. Paper no. TII-18-0025. (Corresponding author: Zhezhuang Xu.)

Z. Xu, R. Wang, X. Yue, and T. Liu are with the School of Electrical Engineering and Automation, Fuzhou University, Fuzhou 350000, China, and also with the Key Laboratory of Industrial Automation Control Technology and Information Processing, the Education Department of Fujian Province, Fuzhou 350000, China (e-mail: zzxu@fzu.edu.cn; wangrk0904@qq.com; yuexi1120@qq.com; liuting922@qq.com).

C. Chen is with the Department of Automation, Shanghai Jiao Tong University, Shanghai 200240, China (e-mail: cailianchen@sjtu.edu.cn).

S.-H. Fang is with the Department of Electrical Engineering, Yuan Ze University, Chung-Li 32003, Taiwan, and also with the MOST Joint Research Center for AI Technology and All Vista Healthcare, Taoyuan 320, Taiwan (e-mail: shfang@saturn.yzu.edu.tw).

Color versions of one or more of the figures in this paper are available online at <http://ieeexplore.ieee.org>.

Digital Object Identifier 10.1109/TII.2018.2829847



Fig. 1. Face-to-machine interaction in the industrial plant.

network via wireless technologies such as WiFi, Bluetooth, and Zigbee. In this circumstance, the mobile industrial human–machine interaction (HMI) becomes popular, which can support the engineer to interact with the machines at any position around them. It greatly improves the efficiency of industrial field works, such as reading sensor data, setting parameters, and manual control.

However, to establish the data connection, the engineer has to remember the identification number (ID) of each machine, and then manually selects the target from a list. Since the machines are densely deployed at 5–30 nodes per 100 m² in the plant, the considerable number of machines generate over-length list, which always results in wrong connection and waste of time in the manual selection.

As shown in Fig. 1, the HMI in the industrial field is typically executed in a *face-to-machine* manner: The engineer should face to the machine during the interaction to ensure the machine works accurately. In this case, the communication between the mobile device and the target machine is line-of-sight, and the target machine is physically proximal to the mobile device. This scenario is quite different from the existing mobile networks [8], [9]. Therefore, how to take advantages of these characteristics to simplify the process of data connection becomes an interesting issue.

The proximity estimation [9]–[11] is a natural solution, which uses received signal strength indicator (RSSI) to detect the scenario when a pair of nodes approach each other closer than a predefined proximity distance. Besides, indoor localization algorithms can estimate the location of the mobile device by WiFi triangulation [12], WiFi fingerprints [13], [14], or a combination of multiple signals processing [15].

However, the industrial HMI network has several unique characteristics that make challenges to the application of

existing algorithms. At first, the machines are densely deployed in the industrial plant. Take the switching room in the 110 kV substation as an example (see Fig. 1), there are 36–48 switch cabinets deployed in the room, and the width of each cabinet is 0.6 m. The estimation error of existing algorithms is greater than 1 m [9], [15] that can hardly satisfy the requirement of estimation accuracy. Second, the engineer has to interact with different machines 5–20 times per hour; thus, the time complexity of the algorithm becomes a significant issue. In related works, the RSSI has to be filtered before estimation due to its fluctuation. The sampling and filtering of RSSI from a large number of machines will generate considerable delay (larger than 12 s) that can hardly be tolerated by the engineer.

It is important to note that the face-to-machine HMI does not demand an absolute position or distance estimation as offered by the previously mentioned algorithms, but rather requires a determination of the machine that is proximal to the mobile device. With its special characteristics and requirements, we aim to propose a proximity estimation algorithm tailored for the face-to-machine HMI. Specifically, our work makes the following contributions.

- 1) We implement a mobile industrial HMI testbed based on Bluetooth to testify the viability of using RSSI to realize the face-to-machine proximity estimation (FaceME). Then, a general model is proposed to formulate the node distribution in the mobile industrial HMI.
- 2) The experimental analysis is provided to verify the non-trivial problem of manual selection in the mobile industrial HMI. Then, the experiments are executed to study the time complexity of the proximity estimation algorithm and the RSSI fluctuation in the face-to-machine HMI. These results are used as the guideline to design the FaceME algorithm.
- 3) The FaceME algorithm is proposed based on RSSI difference to estimate the machine node that is proximal to the human node. Moreover, the two-steps estimation is used in FaceME to reduce the time complexity.
- 4) Theoretical analysis is provided to study the performance of FaceME. Based on the modeling of the time complexity and estimation accuracy in FaceME, an optimization problem is formulated to obtain the optimal RSSI sampling number in different scenarios.
- 5) The experiments are executed to prove the effectiveness of FaceME. The results prove that the FaceME algorithm improves the estimation accuracy and time complexity by comparing with the existing proximity estimation algorithm.

The rest of this paper is organized as follows. Section II provides a brief introduction about related works. Section III introduces the mobile industrial HMI testbed. In Section IV, we use the testbed to study the problem of existing algorithms in the mobile industrial HMI and propose the definition of RSSI difference. Section V presents the details of FaceME algorithm, which is developed based on RSSI difference, then the performance of FaceME is theoretically analyzed in Section VI. The experiment results are given in Section VII to evaluate the

performance of FaceME algorithm. Finally, Section VIII makes the conclusion of this paper.

II. RELATED WORKS

With the development of industrial Internet of things, more and more machines have been connected to the network via wireless technologies such as WiFi and Bluetooth [6], [16]. However, the growing number of nodes becomes a nontrivial problem for the engineers, since they have to remember the IP address of each machine or manually select the target machine from a huge list, which leads to incorrect selection and waste of time.

To simplify the data connection, a straightforward solution is using QR code [17], [18] or NFC [19], [20] scanning to obtain the ID before connection. However, both of them have to be executed in extremely short range (< 20 cm), which cannot be applied in the industrial plant with large or dangerous machines.

Another potential solution is the indoor localization algorithm [21], which can estimate the location of mobile nodes, then the estimated location can be used to identify neighbor machines. In [12], Shu *et al.* proved that RSSI-based triangulation can provide reasonable localization in the indoor environments based on empirical studies. The most commercially adopted solutions use fingerprints of WiFi signals to create WiFi radio map in an offline process, then the online location estimation is performed based on the maps [13], [14]. Some works combine the WiFi signals with smart sensors [15] to improve the localization accuracy.

On the other hand, proximity estimation algorithms [9]–[11], [22], [23] use RSSI to estimate the proximity of a pair of nodes rather than an absolute position. The most popular commercial product that uses the proximity estimation algorithm is the iBeacon developed by Apple. Some works have developed new algorithms based on iBeacon to improve proximity detection accuracy [24], [25]. In [9], Liu *et al.* discussed the face-to-face proximity estimation in the indoor environments, and then propose threshold-based methods to estimate proximity. With the threshold obtained in the offline measurements and the online data smoothing, the estimation accuracy is improved to 1–1.5 m that satisfies the requirement of measuring face-to-face proximity.

The related works prove that RSSI is a reasonable solution to estimate the proximity in the indoor environments. Nevertheless, most of them are developed for the applications in living buildings. The characteristics of mobile industrial HMI have not been considered. The face-to-machine proximity requires the estimation of the proximal node, rather than an absolute location or distance. Moreover, the machine nodes are densely deployed that demands higher estimation accuracy, and the time complexity of the algorithm should be small enough to satisfy the frequent HMI. To satisfy these demands, our solution distinguishes the methods of related works in two aspects: 1) The RSSI difference between the proximal node and other nodes is measured in the offline process rather than the RSSI of the proximal node. 2) The number of nodes involved in RSSI sampling and filtering is controlled based on two-steps estimation to reduce the time complexity. The details of our works are provided in the following sections.

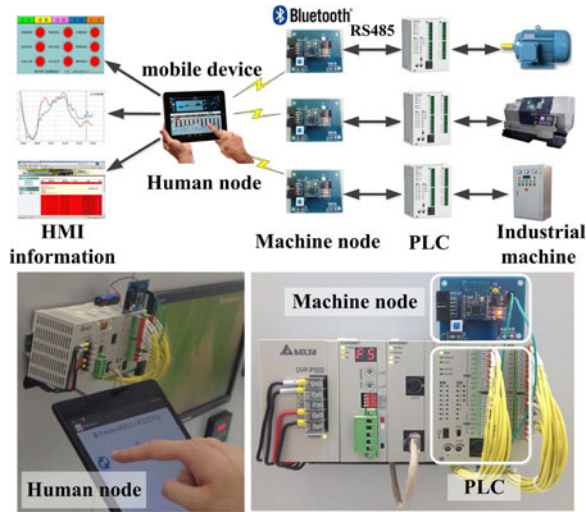


Fig. 2. Framework of the mobile industrial HMI testbed.

III. MOBILE INDUSTRIAL HMI TESTBED AND MODEL

We implement a mobile industrial HMI testbed to evaluate the performance of wireless communication in face-to-machine HMI. As shown in Fig. 2, the testbed consists of three parts: the *human node*, which is defined as the mobile device carried by the engineer, the *machine node*, which is defined as the wireless module integrated with Bluetooth and RS485 communication chips, and the *programmable logic controller (PLC)*, which is the most popular controller in the industry. The human node can read the status and modify the parameters of PLC via Bluetooth communication with machine nodes, while the machine node converts Bluetooth packets to RS485 packets and vice versa. The details are described as follows.

A. Hardware and Software

Google Nexus 9 with Android OS version 5.1 is used as the human node in the testbed. We developed an Android application called *MobileHMI* can read the input signals and control the outputs of PLC. The proximity estimation algorithms are also implemented in *MobileHMI* to collect and process Bluetooth RSSI data from machine nodes.

We develop a wireless module as the machine node that consists of a Bluetooth core board and an extension board. The Bluetooth core board uses a TI-CC2541 chip, and the extension board is composed of power converter and a MAX3485 chip to support RS485 communication. The program that completes the conversion between Bluetooth packets and RS485 packets is written based on the BLE-STACK supported by TI.

The PLC is the DVP12SE series developed by Delta Electronics. Each PLC is connected to a machine node by RS485. The PLC is set as the client in the RS485 network and the data packets use Modbus protocol, such that the system software of PLC can handle the communication with the machine node.

B. Testbed Deployment

The testbed is deployed in the Delta PLC laboratory located in Fuzhou University. As shown in Fig. 3, there are 23 control

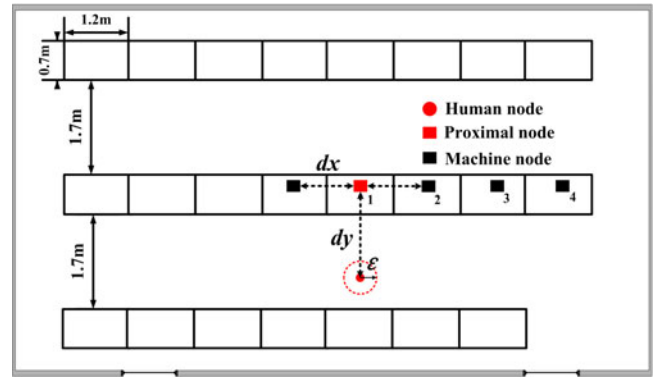


Fig. 3. Layout of the mobile industrial HMI testbed and the node distribution model.

consoles in the laboratory. The size of the laboratory is 12 m \times 7.65 m, and the size of each console is 1.2 m \times 0.7 m.

The testbed represents a typical industrial plant [26], [27]: A large number of machines are deployed in rows with fixed spacing, while the engineer moves in the passage to interact with machines. The HMI is generally executed in a *face-to-machine* manner that the engineer should face to the machine during the interaction to ensure the machine works accurately.

C. Node Distribution Model

In this paper, we define the *proximal node* (denoted as k) as the machine node that is proximal to the human node in the physical space. Since the machines are generally regularly deployed in the plant [26], [27], the network deployment can be formulated by two variables: the spacing among machine nodes dx , and the distance between the human node and the proximal node dy . dx is fixed in the specific industrial plant, while dy is determined by the ideal location of the human node and its safety distance to the machine. Moreover, since the location of the human node is variable due to its mobility, we use a circle with radius ϵ centered at the ideal location of the human node to formulate the randomness of the human node's location. Take the Delta PLC laboratory shown in Fig. 3 as an example, dx is fixed at 1.2 m, and dy is 0.9 m. ϵ is smaller than 0.5 m by considering different operation behaviors.

This model formulates the difference of the distance from the human node to machine nodes, which has great impacts on the values of RSSI and the accuracy of proximity estimation [9]. Due to the powerful hardware of the human node, in this paper, the human node runs the proximity estimation algorithm to sample and process the RSSI of machine nodes. The RSSI of the machine node i is denoted by $R(i)$. The variables used in this paper are summarized in Table I.

IV. PROBLEM STATEMENT

In this section, we first execute experiments to verify the nontrivial problem of manual selecting the proximal machine node from a node list. Then, the problems of using proximity estimation in the face-to-machine HMI are analyzed in two aspects: *time complexity* and *RSSI fluctuation*. The face-to-face

TABLE I
VARIABLES LIST

Variable	Description
dx	the spacing among machine nodes
dy	the distance between human node and proximal node
k	the proximal machine node
M^-	the set of machine nodes scanned by the human node except the proximal machine node
$R(i)$	the RSSI value of machine node i
R_{\max}	the maximum RSSI value scanned by the human node
$\Delta R(k, M^-)$	the RSSI difference
$L(R_1(k))$	the lower bound of the original RSSI value of the proximal node
$U(R_1(M^-))$	the upper bound of the original RSSI value of all nodes in M^-
m	the RSSI sampling number for the filtering algorithm
$L(R_m(k))$	the lower bound of the filtered RSSI value of the proximal node
$U(R_m(M^-))$	the upper bound of the filtered RSSI value of all nodes in M^-

proximity estimation [9], which has been proved to provide the best estimation accuracy in related works, is implemented in our testbed for comparison. In face-to-face proximity estimation, the node with the filtered RSSI is compared with a threshold measured in the offline phase to estimate whether the node is in proximity. The RSSI has to be sampled multiple times before filtering, and the number of sampling times is defined as the sampling number m .

A. Manual Selection

In the face-to-machine HMI, the considerable number of machine nodes makes the manual node selection a nontrivial problem for engineers, especially when they have to make different connection 5–20 times per hour.

To verify this problem, we develop an application on Android to obtain the experimental results. At the beginning, the participant has to touch the start button on the screen, then a random ID is displayed on the top of the screen, followed by a node list with variable number of nodes. The participant has to select the corresponding ID from the list, and finally click the confirm button. The selection time will be recorded as the duration between the time that the participant touches the start button and the time that the confirm button is clicked.

We invite 16 participants that are divided four teams to execute this experiment. The participants in each team take turns to carry out the experiment for 7 times with different length of the list. The length of the list varies from 2 to 20, and the experimental results are given in Table II. It is clear to see that the selection time increases with the growth of the list. When the number of nodes in the list is larger than 20, the selection time is larger than 6 s. Moreover, one wrong selection appears in the experiments, and most participants feel troubled when the list is longer than 12.

The number of nodes is considerable in the dense-deployed plant such as electrical substation. We deploy 23 machine nodes in the Delta PLC laboratory described in Section III-B, and then

TABLE II
MANUAL SELECTION TIME WITH DIFFERENT NUMBER OF NODES IN THE LIST

Number of nodes	Selection Time (ms)
2	2073.45
3	2379.06
4	2458.77
5	2628.02
7	3199.68
12	4328.13
20	6057.92

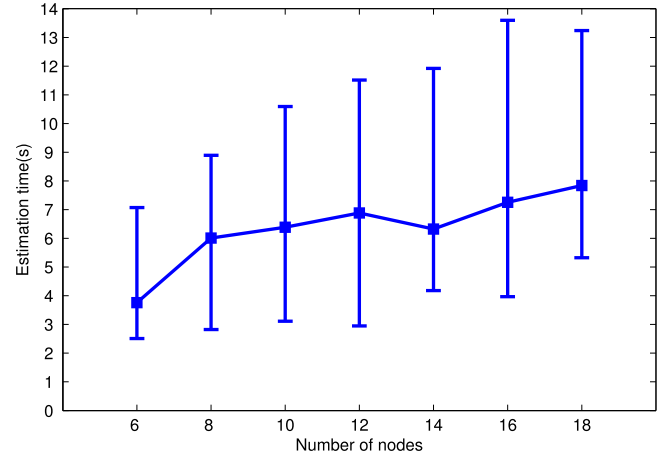


Fig. 4. Estimation time with different node numbers.

use the human node to scan machine nodes at the corners of the laboratory. The results show that all 23 machine nodes can be scanned by the human node. Therefore, using proximity estimation to reduce the complexity of manual selection is important in the industrial internet of things.

B. Time Complexity

The existing proximity estimation algorithm cannot be applied in the face-to-machine HMI directly. The first challenge is the time complexity. We first study how does the number of nodes impact the time complexity of proximity estimation. The machine nodes are deployed with $dx = 1.2$ m and $dy = 0.9$ m. The sampling number of RSSI is fixed at 20, and the advertisement interval of machine nodes is set as 100 ms.

Fig. 4 shows the estimation time when the number of machine nodes (denoted as n) grows from 6 to 18. With the increasing number of nodes, the average estimation time gradually grows from 3.761 to 7.839 s. Moreover, the maximum estimation time grows from 7.073 to 13.599 s, which is approximately more than two times with the average one. The reason is the broadcasting scheme of Bluetooth, which is designed based on carrier sense multiple access (CSMA). The increasing number of nodes leads to the growth of interference, and the random backoff scheme used in CSMA brings the significant variation of estimation time.

In proximity estimation algorithms, the human node generally has to sample the RSSI of machine nodes multiple times, such that the filtering algorithm can be used to smooth the fluctuation

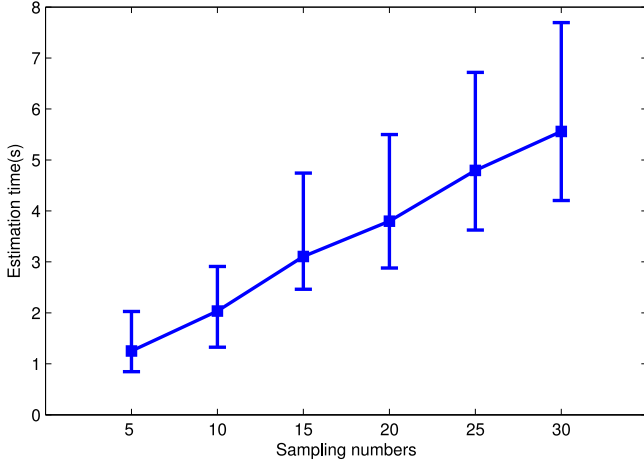


Fig. 5. Estimation time with different sampling numbers.

of RSSI values. Therefore, we study the relationship between the RSSI sampling number (denoted as m) and the estimation time. The number of machine nodes is fixed at 10, and they are deployed with $dx = 1.2$ m and $dy = 0.9$ m in the laboratory.

As shown in Fig. 5, when the sampling number increases from 5 to 30, the average estimation time grows from 1.250 to 5.558 s, and the maximum estimation time grows from 2.026 to 7.694 s. It is because the machine node broadcasts periodically. In this case, the human node has to wait for more broadcast periods with the growth of the sampling number.

To summarize, both the number of machine nodes and the sampling number have great impact on the estimation time. The variation of estimation time is significant, and the maximum estimation time is hard to be tolerant in the industrial HMI application. Moreover, although increasing RSSI sampling number is helpful to improve the estimation accuracy, the cost is the growth of estimation time. These results motives us to design a new proximity estimation algorithm that can guarantee the estimation accuracy with limited estimation time.

C. RSSI Fluctuation

In the face-to-machine HMI, an essential problem is to determine whether the RSSI is sufficient to estimate the proximal machine node. Therefore, we execute an experiment to examine the RSSI of machine nodes in the face-to-machine HMI.

In the experiment, four machine nodes are deployed in the laboratory as shown in Fig. 3. Each machine node is connected to a control console separately; thus, the space among them dx is 1.2 m. The ID of the proximal node is 1. The human node locates in front of the proximal node, and its distance to the proximal node dy is 1.2 m. The human node measures the RSSI of all machine nodes simultaneously at every 10 s, and the measurements are repeated over the period of 35 min.

Fig. 6 shows the fluctuations of RSSI values with all machine nodes. Although the RSSI varies significantly for the same node, its variance is constrained in a limited interval and there is a noticeable gap exists between the proximal node and the other

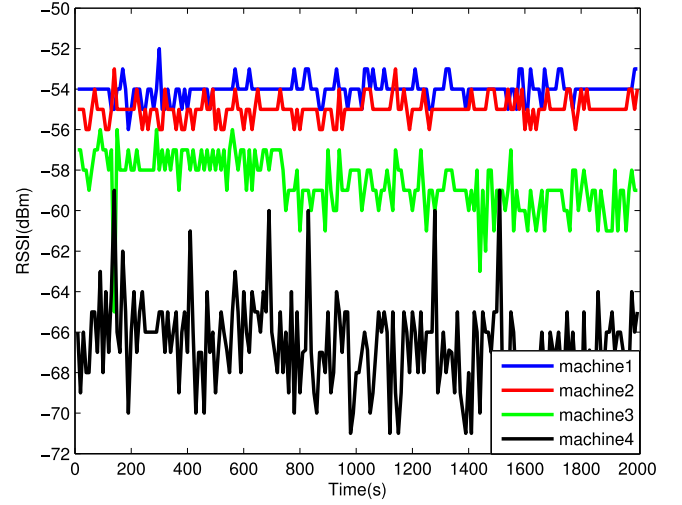


Fig. 6. RSSI of machine nodes with $dx = 1.2$ m and $dy = 1.2$ m.

machine nodes. Such results further shed light on the viability of using RSSI to estimate the proximal node.

On the other hand, as shown in Fig. 6, there are overlap between the RSSI fluctuation interval of machine 1 and 2. It may lead to the wrong estimation of the proximal node. Thus, we further evaluate the RSSI fluctuation based on the log-normal shadowing model [28]

$$R(i) = A - 10\gamma \log(d_i) + X \quad (1)$$

where d_i is the distance between the human node and the machine node i , A is the received power at a reference distance, γ is the path loss exponent, and X reflects the variation of the received power at a certain distance.

The model divides the factors that impact the RSSI into two categories: the deterministic factors and the stochastic factors. The deterministic factors include the distance between two nodes, the setting of radio parameters, and the estimated path loss exponent. The stochastic factors include the hardware heterogeneity, the power volatility, and the variation of channel state [29].

However, this model is not sufficient to formulate the problem in the FaceME. In practice, after RSSI sampling, the human node can obtain a list of machine nodes combining with their RSSI. It is important to note that, the human node can not identify the proximal node k from the list, but rather obtain the node with the maximum RSSI R_{\max} . In this case, the accuracy of proximity estimation depends on the relations between $R(k)$ and R_{\max} . Therefore, the maximum and minimum values of RSSI are more important than the mean value and variance. This result motivates us to propose the definition of RSSI difference.

D. RSSI Difference

In this section, we provide the formal definition of RSSI difference, and then discuss its relations with the FaceME.

At first, we formulate the fluctuation of $R(i)$ as

$$R(i) \in [L(R(i)), U(R(i))] \quad (2)$$

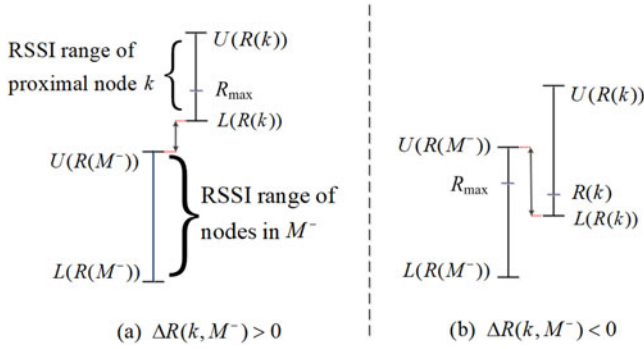


Fig. 7. Two cases of RSSI Difference.

where $L(R(i))$ is the lower bound of $R(i)$, and $U(R(i))$ is the upper bound of $R(i)$.

The set of machine nodes that can be detected by the human node is denoted by M , and the proximal node is denoted by k . Then, we define the set of machine nodes M^- as

$$M^- = \{i | (i \in M) \cap (i \neq k)\}. \quad (3)$$

Given the set of nodes M^- , the RSSI difference $\Delta R(k, M^-)$ is defined as

$$\Delta R(k, M^-) = L(R(k)) - U(R(M^-)). \quad (4)$$

The definition of the RSSI difference $\Delta R(k, M^-)$ indicates the difference between the lower bound of $R(k)$ and the upper bound of $R(M^-)$. Next, we will discuss the relations between the accuracy of proximity estimation and the RSSI difference $\Delta R(k, M^-)$.

Fig. 7 demonstrates two different cases of RSSI difference. If $\Delta R(k, M^-) \geq 0$, which means the minimum RSSI of the proximal node is larger than the maximum RSSI of any other nodes, the node that has the maximum RSSI R_{\max} will be destined to be the proximal node. Otherwise, if $\Delta R(k, M^-) < 0$, there will be overlap between the RSSI fluctuation interval of k and M^- . In this case, R_{\max} may not be equal to $R(k)$, which could result in estimation error.

To clarify the analysis, we formally derive the relations between $R(k)$ and R_{\max} as follows.

Theorem 1: Given the RSSI of the proximal node $R(k)$ and the maximum RSSI of all machine nodes R_{\max} , if $\Delta R(k, M^-) < 0$, then

$$R(k) \in [R_{\max} + \Delta R(k, M^-), R_{\max}]. \quad (5)$$

Otherwise, if $\Delta R(k, M^-) \geq 0$, then $R(k) = R_{\max}$.

Proof: At first, we consider the condition when $\Delta R(k, M^-) < 0$. Assume that the node j , which has $R(j) = R_{\max}$, combining with (2) and (4), we have

$$\begin{aligned} R(k) &\geq L(R(k)) \\ &= U(R(M^-)) + \Delta R(k, M^-) \\ &\geq R_{\max} + \Delta R(k, M^-) \end{aligned} \quad (6)$$

then (5) can be easily derived based on (6).

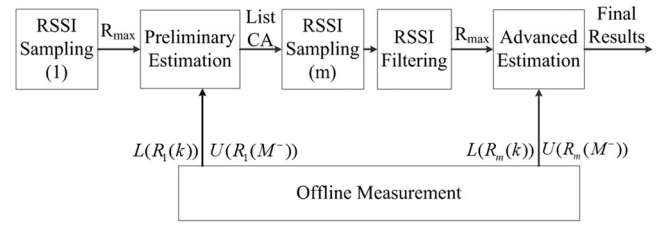


Fig. 8. Framework of FaceME algorithm.

When $\Delta R(k, M^-) \geq 0$, we can derive

$$\begin{aligned} R(k) &\geq L(R(k)) \\ &= U(R(M^-)) + \Delta R(k, M^-) \\ &\geq R(i) + \Delta R(k, M^-) \geq R(i), i \in M^- \end{aligned} \quad (7)$$

which means that $R(k)$ is guaranteed to be larger than the RSSI of any other nodes. Therefore, $R(k) = R_{\max}$.

Theorem 1 provides an in-depth view of the factors that impact the estimation accuracy. At first, a sufficient condition to guarantee the estimation accuracy can be derived directly from Theorem 1

$$\Delta R(k, M^-) \geq 0. \quad (8)$$

This condition depicts that the growth of $\Delta R(k, M^-)$ is helpful to improve the estimation accuracy. Combining the RSSI model (1) with the node distribution model given in Section III-C, the estimation accuracy is better in the network with larger dx or smaller dy . On the other hand, the filtering algorithm and increasing the RSSI sampling number can improve the estimation accuracy.

Moreover, although the network with large number of the node can generate numerous data of RSSI, only $L(R(k))$ and $U(R(M^-))$ is related to the estimation accuracy. This result is helpful to reduce the complexity of the offline phase in the proximity estimation. We will use these results to design the FaceME algorithm described in Section V.

V. FACE-TO-MACHINE PROXIMITY ESTIMATION

In this section, we describe the details of the FaceME algorithm. The basic idea of FaceME is using RSSI difference, specifically $L(R(k))$ and $U(R(M^-))$, to estimate the proximal node. Moreover, the two-steps estimation is executed to reduce the number of RSSI sampling, and hence, reduce the time complexity of the algorithm.

Fig. 8 demonstrates the framework of FaceME algorithm that includes two parts: the offline measurement to obtain $L(R(k))$ and $U(R(M^-))$ and the online estimation that uses $L(R(k))$ and $U(R(M^-))$ and sampling results for proximity estimation. The online estimation is further separated into preliminary estimation and advanced estimation. The preliminary estimation uses $L(R(k))$ and $U(R(M^-))$ to reduce the number of machine nodes that is involved in the advanced estimation, while the advanced estimation combines RSSI filtering and $L(R(k))$ and $U(R(M^-))$ to derive the final estimation result. The details of FaceME algorithm are described as follows.

A. Offline Measurement

The goal of the offline measurement is to obtain $L(R(k))$ of the proximal node and $U(R(M^-))$ of other nodes influenced by dx and dy . dx is fixed in the specific industrial plant, while dy is variable due to the mobility of the human node. Therefore, in the offline measurement, the human node should locate in front of the proximal node with different dx and dy and sample the RSSI from every machine nodes, then it can obtain $L(R(k))$ and $U(R(M^-))$.

To support the online estimation, the offline measurement is required to obtain $L(R(k))$ and $U(R(M^-))$ after the RSSI values are processed by the filtering algorithm. Specifically, $L(R_1(k))$ and $U(R_1(M^-))$ are defined as the result without being processed by filtering algorithm, and $L(R_m(k))$ and $U(R_m(M^-))$ are defined as the result that is filtered with the sampling number m . The value of $L(R_1(k))$, $U(R_1(M^-))$ and $L(R_m(k))$, $U(R_m(M^-))$ will be used in the online estimation.

Any filtering algorithm [25], [30] can be used in FaceME to process RSSI. Considering the characteristics of wireless communication in the face-to-machine HMI, in this paper, the RSSI is processed based on Gaussian filter. Gaussian filter is the linear smoothing filter to select the values, which locate in the large distribution density of the Gaussian model and delete the values caused by small probability event. The value of RSSI follows Gaussian distribution $N(\mu, \sigma^2)$ [31]. The density function is described as

$$f(\text{RSSI}) = \frac{1}{\sigma\sqrt{2\pi}} e^{-\frac{(\text{RSSI}-\mu)^2}{2\sigma^2}} \quad (9)$$

where

$$\mu = \frac{1}{m} \sum_{j=1}^m \text{RSSI}_{(j)} \quad (10)$$

$$\sigma = \sqrt{\frac{1}{m-1} \sum_{j=1}^m (\text{RSSI}_{(j)} - \mu)^2} \quad (11)$$

where the parameter μ is the mean value of RSSI and σ is the standard deviation of RSSI. $\text{RSSI}_{(j)}$ denotes the value of RSSI in the j th measurement and m is the RSSI sampling number required for the filter algorithm. Then, the high probability interval of RSSI can be formulated as

$$\text{RSSI} \in [\mu - \sigma, \mu + \sigma]. \quad (12)$$

The number of RSSI filtered in the high-probability interval is described as N_R . Then, we average all the filtered RSSI values to derive the final result, which is formulated as

$$\overline{\text{RSSI}} = \frac{1}{N_R} \sum_{j=1}^{N_R} \text{RSSI}_{(j)}. \quad (13)$$

In this paper, the filtering algorithm described above is used in the offline measurement and online estimation of FaceME to smooth RSSI fluctuation.

B. Online Estimation

The online estimation consists of preliminary estimation and advanced estimation. In the preliminary estimation, the human node samples the RSSI of each machine node only once. The human node can obtain $R_{\max}(1)$ and a neighbor list from the sampling results. Then, $R_{\max}(1)$ and $L(R_1(k))$, $U(R_1(M^-))$ obtained in the offline measurement is used to remove redundant nodes. The human node first checks if $R_{\max}(1) > U(R_1(M^-))$. If yes, the node that has $R_{\max}(1)$ can be directly estimated as the proximal node. Otherwise, the human node checks the RSSI of all nodes in the neighbor list, keeps the node that satisfies $R_1(i) \in [L(R_1(k)), R_{\max}(1)]$, and removes the other nodes. The remaining nodes compose the proximal candidates list called CA.

If there is only one node in the CA list, this node is destined to be the proximal node. Otherwise, it means the human node is unable to accurately estimate the proximal node. Then, the advanced estimation will be executed based on the CA list.

In the advanced estimation, the RSSI of nodes in the CA list should be further sampled for m times. Then, the RSSI is processed by Gaussian filter to reduce its fluctuation, and the maximum value of the filtered RSSI $R_{\max}(m)$ can be obtained. Combining with $L(R_m(k))$ and $U(R_m(M^-))$ obtained in the offline measurement, the human node can remove redundant nodes from the CA list. If $R_{\max}(m) > U(R_m(M^-))$, the node that has $R_{\max}(m)$ can be directly estimated as the proximal node. Otherwise, the human node checks the filtered RSSI of all nodes in the CA list, keeps the node that satisfies $R_m(i) \in [L(R_m(k)), R_{\max}(m)]$, and removes the other nodes.

After processing all the nodes in the CA list, the human node obtains the final estimation result. If only one node is left in the estimation result, the human node will directly connect to it. On the other hand, if there are more than one node in the estimation results, their ID will be displayed in the user interface for manual selection.

C. Adaptation for Variable Environment

The framework of FaceME algorithm is easy to be implemented in the industrial field. Nevertheless, $L(R(k))$ and $U(R(M^-))$ may be variable due to the human mobility, hardware heterogeneity, power volatility, and variation of channel state. Therefore, how to obtain reasonable $L(R(k))$ and $U(R(M^-))$ in variable environment is a challenging issue.

The problem can be solved in both offline measurement and online estimation. Massive offline measurement in variable industrial environment can be executed to generate a database of $L(R(k))$ and $U(R(M^-))$. In a specific industrial field, $L(R(k))$ and $U(R(M^-))$ can be selected from the database according to the user setting (such as dx and dy) and test estimation. It is important to note that, the offline measurement can be done by the manufacturer before implementation. Therefore, the offline measurement is not the burden for the users.

Moreover, the adaptive setting of $L(R(k))$ and $U(R(M^-))$ can be adopted in the online estimation. If the proximal node is not included in the estimation result, the user can input the

feedback, then the human node will display the nodes that are not included in the estimation result. Once the user selects the proximal node, the algorithm can recalculate $L(R(k))$ and $U(R(M^-))$ then use it for future estimation. On the other hand, if the setting of $L(R(k))$ is so large or $U(R(M^-))$ is so small that there are too many nodes in every estimation result, $L(R(k))$ and $U(R(M^-))$ can also be **recalculated** for future estimation. The adaptive setting of RSSI difference is an interesting problem, which may greatly improve the efficiency of FaceME. We will investigate this problem in future works.

VI. THEORETICAL ANALYSIS

In this section, the theoretical analysis is provided to evaluate the performance of FaceME including its time complexity and estimation accuracy, and further discuss how to determine the RSSI sampling number by formulating an optimization problem.

A. Time Complexity

According to the experimental results shown in Figs. 4 and 5, the time complexity has tight relations with the RSSI sampling number (m) and the number of nodes involved in RSSI sampling (n). Based on the research works of latency in the neighbor discovery of BLE [32], [33], the time complexity of RSSI sampling can be estimated as

$$t(n, m) = (\alpha \cdot T_{\text{adv}} + T_{\text{pro}}) \cdot e^{\beta \cdot \frac{n}{\alpha \cdot T_{\text{adv}} + T_{\text{pro}}}} \cdot m \quad (14)$$

where T_{adv} is the advertisement interval of machine nodes, and T_{pro} denotes the processing time for neighbor discovery. α and β are the coefficients that mainly depends on the hardware of the human node.

In FaceME, the online estimation is divided into preliminary estimation and advanced estimation. In the preliminary estimation, the human node scans the RSSI of all neighbor machine nodes only once (no RSSI filtering). In the advanced estimation, only the RSSI of the nodes in the CA list will be sampled m times. Then, we can estimate the time complexity in the online estimation as

$$T_e = \begin{cases} t(n_1, 1) & n_2 = 1 \\ t(n_1, 1) + t(n_2, m) & n_2 > 1 \end{cases} \quad (15)$$

where n_1 is the number of all machine nodes that can be scanned by the human node, and n_2 denotes the number of nodes in the list CA after preliminary estimation.

According to our experiments given in Section IV-A, in the room smaller than 100 m², the n_1 can be approximated as the number of *all* nodes. Then, we discuss how to estimate n_2 . To clarify the analysis, we only consider the scenario that the proximal node is successfully contained in the estimation results.

In the preliminary estimation of FaceME, if $R_{\text{max}} > U(R_1(M^-))$, the node that has R_{max} will be estimated as the proximal node directly, thus, $n_2 = 1$. Otherwise, the node that has $R_1(i) \in [L(R_1(k)), U(R_1(M^-))]$ will be contained in the

estimation results. Therefore, the expectation of n_2 is

$$\begin{aligned} E(n_2) &= P\{R_1(k) > U(R_1(M^-))\} \\ &\quad + P\{R_1(k) < U(R_1(M^-))\} \\ &\quad \times \sum_{i \in M^-} P\{R_1(i) \in [L(R_1(k)), U(R_1(M^-))]\}. \end{aligned} \quad (16)$$

$U(R_1(M^-))$ and $L(R_1(k))$ can be obtained in the offline measurement. With the distance d_i between the machine node i and the human node, the probability can be calculated based on the log-normal shadowing model [28]

$$R(i) = A - 10\gamma \log(d_i) + X \quad (17)$$

where A is the received power at a reference distance, γ is the path loss exponent, and X reflects the variation of the received power that follows Gaussian distribution. All of them can be estimated based on the data gathered in the offline measurement of FaceME.

B. Estimation Accuracy

In FaceME, the estimation accuracy can be measured in two aspects: the **probability that the proximal node is included in the estimation results P_k** , and the **number of nodes in the estimation results n_3** . According to the algorithm, the proximal node is guaranteed to be in the estimation results if its RSSI is larger than the $L(R(k))$ obtained in the offline measurement. Therefore, the P_k can be estimated by

$$P_k = P\{R_1(k) \geq L(R_1(k))\} * P\{R_m(k) \geq L(R_m(k))\}. \quad (18)$$

Similar to the n_2 given in (16), the number of nodes in the final estimation result n_3 can be estimated as

$$\begin{aligned} E(n_3) &= P\{R_m(k) > U(R_m(M^-))\} \\ &\quad + P\{R_m(k) < U(R_m(M^-))\} \\ &\quad \times \sum_{i \in M_{\text{CA}}} P\{R_m(i) \in [L(R_m(k)), U(R_m(M^-))]\} \end{aligned} \quad (19)$$

where M_{CA} denotes the set of machine nodes in the list CA, i.e., the preliminary estimation results.

It is worth to note that the RSSI sampling number m has great impact on n_3 . The main reason is that the filtering algorithm is helpful to smooth the RSSI fluctuation, and the variation of the RSSI σ reduces with the growth of the sampling number m . The relation can be formulated as

$$\sigma = \frac{a}{m + b} \quad (20)$$

where a and b are the coefficients that varies in different node deployment.

C. RSSI Sampling Number

Based on the analysis given above, there is a tradeoff in the complexity of FaceME and manual selection: Increasing the RSSI sampling number m is helpful to reduce the number of nodes in the estimation results n_3 . On the other hand, it results in the growth of time in the advanced estimation T_e . Thus, we

can formulate an optimization problem to determine the value of RSSI sampling number m in different scenarios.

A key challenge in formulating the optimization problem is that the metrics to measure time complexity (T_e) and estimation accuracy (P_k and n_3) are different. Motivated by the manual selection experiment given in Section IV-A, we propose a variable T_s to formulate the time complexity in the manual selection

$$T_s = \begin{cases} 0 & n_3 = 1 \\ \tau_1 \cdot n_3 + \tau_2 & n_3 > 1 \end{cases} \quad (21)$$

where $\tau_1 \cdot n_3$ denotes the time for searching the target ID, and τ_2 is the time for selecting the target. Both of them are determined by the complexity of the user interface on the human node, and they can be easily obtained in experiments. Based on the experimental results given in Section IV-A, $\tau_1 = 247.6$ ms and $\tau_2 = 1491.5$ ms. When $n_3 = 1$, the human node can automatically connect to the proximal node without manual selection, thus, $T_s = 0$.

With the help of T_s , we propose the metric called composite estimation time \mathcal{T} that considers the time complexity and estimation accuracy simultaneously.

$$\mathcal{T} = \lambda \cdot T_e + (1 - \lambda) \cdot T_s \quad (22)$$

where λ is a coefficient to control the weight of time complexity and manual selection. It is important to note that reducing n_3 not only decreases the time of manual selection T_s , but also reduces the burden for engineers and the probability of wrong manual selection. Therefore, λ is generally in $[0.1, 0.5]$ that emphasizes simplifying the manual selection.

Based on the discussion given above, the RSSI sampling number m can be obtained by solving the following optimization problem:

$$\begin{aligned} & \text{minimize} && \mathcal{T} \\ & \text{subject to} && P_k > \theta \\ & && \mathcal{T}(m) = \lambda \cdot T_e + (1 - \lambda) \cdot T_s \\ & && m = 1, 2, 3, \dots \end{aligned}$$

where θ is a parameter to control the demand of estimation accuracy, which is generally larger than 95%.

VII. EXPERIMENTAL EVALUATION

In this section, we execute experiments to evaluate the performance of FaceME. For comparison, the Face-to-face proximity estimation [9] is also implemented in the testbed. The experiments are executed in the Delta PLC laboratory shown in Fig. 3. Each experiment runs 100 times, and the statistic results are demonstrated in the following sections.

A. Estimation Time

The estimation time of FaceME algorithm with face-to-face proximity estimation are compared in this section. dx is set as 0.9 m, and dy is fixed at 1.2 m. The number of machine nodes grows from 6 to 18. The RSSI sampling number m is fixed at 20, and the broadcast period of machine nodes is set at 100 ms.

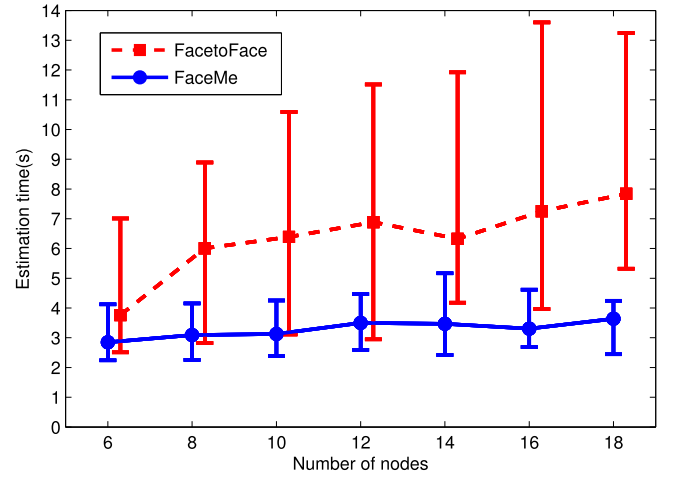


Fig. 9. Estimation time comparison.

TABLE III
NUMBER OF NODES IN THE CA LIST (FACEME)

$\frac{dy}{dx}$	0.9	1.2	1.5	1.8
0.6	1 : 93% 2 : 7%	1 : 99% 2 : 1%	3 : 31% 4 : 25% 5 : 44%	1 : 8% 2 : 52% 3 : 39% 4 : 1%
0.9	1 : 94% 2 : 6%	1 : 33% 2 : 1% 3 : 66%	1 : 75% 2 : 25%	1 : 41% 2 : 19% 3 : 40%
1.2	1 : 100%	1 : 100%	1 : 19% 2 : 23% 3 : 58%	2 : 31% 3 : 66% 4 : 3%

As shown in Fig. 9, FaceME has great improvement in the estimation time T_e . In FaceME, the average estimation time ranges in 2.849–3.638 s, and the maximum estimation time ranges in 4.123–5.166 s. On the other hand, in face-to-face proximity estimation, the average estimation time grows from 3.761 to 7.839 s, and the maximum estimation time grows from 7.008 to 13.599 s. Compared with face-to-face proximity estimation, FaceME greatly reduces the estimation time from 24.26% to 53.59%. According to Section V, the preliminary estimation of FaceME uses RSSI difference to reduce the number of nodes that involve in the advanced estimation and, thus, reduces the estimation time.

To prove the effectiveness of the preliminary estimation, the number of nodes in the CA list is further analyzed. The number of all machine nodes is fixed at 18. dx varies from 0.6 to 1.2 m, and dy grows from 0.9 to 1.8 m. The results are given in Table III. The numbers in the table indicate the number of nodes in the CA list, and the percentage that follows each number demonstrates the frequency that each number appears in the experiments.

TABLE IV
NUMBER OF NODES IN THE ESTIMATION RESULTS

$\begin{matrix} dy \\ dx \end{matrix}$	0.9		1.2		1.5		1.8	
	FaceME	FacetoFace	FaceME	FacetoFace	FaceME	FacetoFace	FaceME	FacetoFace
0.6	1 : 100%	1 : 72% 2 : 28%	1 : 100%	1 : 99% 2 : 1%	2 : 5% 3 : 55% 4 : 16% 5 : 24%	2 : 5% 3 : 50% 4 : 20% 5 : 25%	1 : 45% 2 : 54% 3 : 1%	1 : 9% 2 : 84% 3 : 7%
0.9	1 : 100%	1 : 93% 2 : 7%	1 : 41% 2 : 5% 3 : 54%	1 : 99% 2 : 1% 3 : 83%	1 : 100%	1 : 83% 2 : 17%	1 : 77% 2 : 9% 3 : 14%	1 : 60% 2 : 14% 3 : 26%
1.2	1 : 100%	1 : 100%	1 : 100%	1 : 100%	1 : 28% 2 : 24% 3 : 48%	1 : 14% 2 : 23% 3 : 63%	1 : 13% 2 : 87%	1 : 4% 2 : 96%

As shown in Table III, the maximal number of nodes is 5, which is greatly reduced by comparing with 18. The fewer number of nodes in the CA list, the less estimation time will consume in the advanced estimation. This result proves the analysis given in Section VI-A.

B. Estimation Accuracy

The estimation accuracy is measured by two metrics: 1) the percentage that the proximal node is contained in the estimation result; 2) the number of nodes in the estimation result. The number of machine nodes is fixed at 18. dx varies from 0.6 to 1.2 m and dy grows from 0.9 to 1.8 m, and the sampling number $m = 10$. The experimental results are recorded in Table IV.

The experiment result shows that all proximal node is guaranteed to be contained in the estimation results in both two algorithms, which means that those two algorithms have the same estimation accuracy $P_k = 100\%$. However, FaceME and face-to-face have great difference in the number of nodes in the final estimation results. The results are given in Table IV. The numbers in the table indicate the number of nodes in the estimation results, and the percentage that follows each number demonstrates the frequency that each number appears in the experiments. It is better to have fewer nodes in the estimation result, which can reduce the complexity for manual selection.

Comparing the results of FaceME and face-to-face in Table IV, we can see that FaceME performs better than face-to-face with all dx and dy . When $dy \leq 1.2$ m, the estimation result of FaceME only has one node, which is destined to be the proximal node. On the other hand, when $dy \geq 1.5$ m, although both algorithms have more than two nodes in the list, the FaceME algorithm has a great advantage in reducing the number of nodes in the estimation result. The major reason is that FaceME considers both $L(R(k))$ and $U(R(M^-))$ in the estimation. These results prove that FaceME is a reasonable solution for FaceME in most applications.

C. Variable Location of the Human Node

As we mentioned in Section III-C, the location of the human node is variable due to its mobility. The human node can

TABLE V
NUMBER OF NODES IN THE ESTIMATION RESULTS WITH VARIABLE LOCATIONS OF THE HUMAN NODE

ε	Left/Right shift		Forward/Backward shift	
	FaceME	FacetoFace	FaceME	FacetoFace
-0.3	1 : 66% 2 : 14% 3 : 20%	1 : 54% 2 : 22% 3 : 24%	1 : 100%	1 : 94% 2 : 6%
-0.2	1 : 80% 2 : 20%	1 : 26% 2 : 74%	1 : 72% 2 : 28%	1 : 50% 2 : 50%
-0.1	1 : 100%	1 : 54% 2 : 46%	1 : 100%	1 : 80% 2 : 20%
0	1 : 52% 2 : 6% 3 : 42%	2 : 16% 3 : 84%	1 : 52% 2 : 6% 3 : 42%	2 : 16% 3 : 84%
+0.1	1 : 100%	1 : 100%	1 : 90% 2 : 10%	1 : 78% 2 : 22%
+0.2	1 : 100%	1 : 100%	1 : 58% 2 : 42%	1 : 30% 2 : 70%
+0.3	1 : 100%	1 : 100%	1 : 100%	1 : 84% 2 : 16%

not locate precisely in the ideal location in practice. Therefore, we execute experiments to analyze the estimation accuracy of FaceME when the location of the human node has a variance ε to the ideal location. dx is fixed at 0.9 m and the original dy is set as 1.2 m. Based on the ideal location, the human node is shifted from 0.1 to 0.3 m in the four directions, respectively. In Table V, the “-” means the left and forward shift, while the “+” denotes the right and backward shift.

The experiment results show that, FaceMe performs better no matter what location the human node is. Moreover, the performance of the proximity estimation algorithms are different at different locations. Specifically, when the human node shifts right from 0.1 to 0.3 m, the algorithms can estimate the proximal node directly. This phenomenon may be generated by the

hardware design of the human node. The reason will be further exploited in future works.

VIII. CONCLUSION

In this paper, the FaceME algorithm is designed based on the RSSI difference to improve the efficiency of data connection in mobile industrial HMI. The mobile industrial HMI testbed is implemented to evaluate the performance of FaceME. The theoretical analysis is provided to analyze the time complexity and estimation accuracy, then an optimization problem is formulated to obtain the optimal RSSI sampling number. The experimental results prove that the FaceME algorithm can provide guaranteed accuracy and low time complexity that satisfies the requirements of the mobile industrial HMI.

REFERENCE

- [1] A. A. Kumar Somappa, K. Øvsthus, and L. M. Kristensen, "An industrial perspective on wireless sensor networks—A survey of requirements, protocols, and challenges," *IEEE Commun. Surveys Tuts.*, vol. 16, no. 3, pp. 1391–1412, Third Quarter 2014.
- [2] F. Lin, C. Chen, N. Zhang, X. Guan, and X. Shen, "Autonomous channel switching: Towards efficient spectrum sharing for industrial wireless sensor networks," *IEEE Internet Things J.*, vol. 3, no. 2, pp. 231–243, Apr. 2016.
- [3] F. Dobsław, T. Zhang, and M. Gidlund, "QOS-aware cross-layer configuration for industrial wireless sensor networks," *IEEE Trans. Ind. Informat.*, vol. 12, no. 5, pp. 1679–1691, Oct. 2016.
- [4] Z. Xu, L. Chen, C. Chen, and X. Guan, "Joint clustering and routing design for reliable and efficient data collection in large-scale wireless sensor networks," *IEEE Internet Things J.*, vol. 3, no. 4, pp. 520–532, Aug. 2016.
- [5] C. Chen, J. Yan, N. Lu, Y. Wang, X. Yang, and X. Guan, "Ubiquitous monitoring for industrial cyber-physical systems over relay-assisted wireless sensor networks," *IEEE Trans. Emerg. Topics Comput.*, vol. 3, no. 3, pp. 352–362, Sep. 2015.
- [6] R. Rondón, M. Gidlund, and K. Landernäs, "Evaluating bluetooth low energy suitability for time-critical industrial IoT applications," *Int. J. Wireless Inf. Netw.*, vol. 24, no. 3, pp. 278–290, Sep. 2017.
- [7] L. Lyu, C. Chen, S. Zhu, and X. Guan, "5G enabled co-design of energy-efficient transmission and estimation for industrial IoT systems," *IEEE Trans. Ind. Informat.*, to be published.
- [8] Z. Su, Q. Xu, and Q. Qi, "Big data in mobile social networks: A QOE-oriented framework," *IEEE Netw.*, vol. 30, no. 1, pp. 52–57, Jan. 2016.
- [9] S. Liu, Y. Jiang, and A. Striegel, "Face-to-face proximity estimation using bluetooth on smartphones," *IEEE Trans. Mobile Comput.*, vol. 13, no. 4, pp. 811–823, Apr. 2014.
- [10] S. Lakshmi Priya and V. Gowthaman, "Improving proximity evaluation for smartphone via bluetooth," *Int. J. Eng. Tech. Sci.*, vol. 2, no. 3, pp. 82–86, 2015.
- [11] J. Y. Jung, D. O. Kang, J. H. Choi, and C. S. Bae, "D2d distance measurement using kalman filter algorithm for distance-based service in an office environment," in *Proc. Int. Conf. Adv. Commun. Technol.*, 2015, pp. 221–224.
- [12] A. Awad, T. Frunzke, and F. Dressler, "Adaptive distance estimation and localization in WSN using RSSI measures," in *Proc. Euromicro Conf. Digit. Syst. Des. Arch., Methods Tools*, 2007, pp. 471–478.
- [13] Y. Shu et al., "Gradient-based fingerprinting for indoor localization and tracking," *IEEE Trans. Ind. Electron.*, vol. 63, no. 4, pp. 2424–2433, Apr. 2016.
- [14] X. Tian, W. Li, Y. Yang, Z. Zhang, and X. Wang, "Optimization of fingerprints reporting strategy for wlan indoor localization," *IEEE Trans. Mobile Comput.*, vol. 17, no. 2, pp. 390–403, Feb. 2018.
- [15] Z. Chen, H. Zou, H. Jiang, Q. Zhu, Y. C. Soh, and L. Xie, "Fusion of wifi, smartphone sensors and landmarks using the kalman filter for indoor localization," *Sensors*, vol. 15, no. 1, pp. 715–732, 2015.
- [16] F. Barac, S. Caiola, M. Gidlund, E. Sisinni, and T. Zhang, "Channel diagnostics for wireless sensor networks in harsh industrial environments," *IEEE Sensors J.*, vol. 14, no. 11, pp. 3983–3995, Nov. 2014.

- [17] H. Zhang, C. Zhang, W. Yang, and C. Y. Chen, "Localization and navigation using QR code for mobile robot in indoor environment," in *Proc. IEEE Int. Conf. Robot. Biomimetics*, 2015, pp. 2501–2506.
- [18] M. Nowicki, M. Rostkowska, and P. Skrzypczyski, "Indoor navigation using QR codes and wifi signals with an implementation on mobile platform," in *Proc. Signal Process., Algorithms, Arch., Arrangements, Appl.*, Sep. 2016, pp. 156–161.
- [19] R. Ramanathan and J. Imtiaz, "NFC in industrial applications for monitoring plant information," in *Proc. Int. Conf. Comput. Commun. Netw. Technol.*, 2013, pp. 1–4.
- [20] L. Tamazirt, F. Alilat, and N. Agoulmine, "NFC-based ubiquitous monitoring system for e-industry," in *Proc. 3rd Int. Conf. Mobile Secure Serv.*, Feb. 2017, pp. 1–4.
- [21] A. Yassin et al., "Recent advances in indoor localization: A survey on theoretical approaches and applications," *IEEE Commun. Surveys Tuts.*, vol. 19, no. 2, pp. 1327–1346, Second Quarter 2017.
- [22] C. Chen, S. Zhu, X. Guan, and X. Shen, *Distributed Consensus Estimation of Wireless Sensor Networks*. Cham, Switzerland: Springer International Publishing, 2014.
- [23] T. Liu, Z. Xu, R. Wang, H. Jiang, C. Chen, and S. H. Fang, "Face-to-machine proximity estimation for mobile industrial human machine interaction," in *Proc. IEEE Int. Conf. Commun.*, May 2017, pp. 1–6.
- [24] H. Zou, H. Jiang, Y. Luo, J. Zhu, X. Lu, and L. Xie, "Bluedetect: An ibeacon-enabled scheme for accurate and energy-efficient indoor-outdoor detection and seamless location-based service," *Sensors*, vol. 16, no. 2, pp. 1–18, Art. no. 268, 2016.
- [25] F. Zafari, I. Papapanagiotou, M. Devetsikiotis, and T. J. Hacker, "Enhancing the accuracy of ibeacons for indoor proximity-based services," in *Proc. IEEE Int. Conf. Commun.*, May 2017, pp. 1–7.
- [26] S. Moazzem, "Performance of spinning plants with facility layout design," in *Proc. IEEE Comput. Eng. Technol. Int. Conf.*, 2010, pp. 36–40.
- [27] W. Li-fang, K. Fan-Sen, C. Jing-hua, and L. Jian-sha, "A new optimization scheme based logistics cost for plant facility layout," in *Proc. World Autom. Congr. 2012*, Jun. 2012, pp. 1–4.
- [28] T. S. Rappaport, *Wireless Communications: Principles and Practice*. Englewood Cliffs, NJ, USA: Prentice-Hall, 1996.
- [29] F. Barac, M. Gidlund, and T. Zhang, "Ubiquitous, yet deceptive: Hardware-based channel metrics on interfered WSN links," *IEEE Trans. Veh. Technol.*, vol. 64, no. 5, pp. 1766–1778, May 2015.
- [30] K. Zhang, Y. Zhang, and S. Wan, "Research of RSSI indoor ranging algorithm based on gaussian—Kalman linear filtering," in *Proc. IEEE Adv. Inf. Manage. Commun., Electron. Autom. Control Conf.*, Oct. 2016, pp. 1628–1632.
- [31] Z. Jianyong, L. Haiyong, C. Zili, and L. Zhaohui, "RSSI based bluetooth low energy indoor positioning," in *Proc. Int. Conf. Indoor Positioning Indoor Navigat.*, Oct. 2014, pp. 526–533.
- [32] J. Liu, C. Chen, and Y. Ma, "Modeling neighbor discovery in bluetooth low energy networks," *IEEE Commun. Lett.*, vol. 16, no. 9, pp. 1439–1441, Sep. 2012.
- [33] J. J. Treurniet, C. Sarkar, R. V. Prasad, and W. D. Boer, "Energy consumption and latency in BLE devices under mutual interference: An experimental study," in *Proc. Int. Conf. Future Internet Things Cloud*, 2015, pp. 333–340.



Zhezhuang Xu (S'10–M'14) received the B.Eng. degree in automation from Xiamen University, Xiamen, China, in 2005, the M.Eng. degree in measuring and testing technologies and instruments from Jiangsu University, Zhenjiang, China, in 2008, and the Ph.D. degree in control science and engineering from Shanghai Jiao Tong University, Shanghai, China, in 2012.

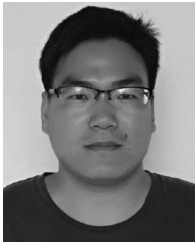
In 2012, he was with the School of Electrical Engineering and Automation, Fuzhou University, Fuzhou, China, where he is currently an Associate Professor. He is the Director of the Public Platform of Industrial Big Data Application, Fujian Provincial Commission of Economy and Information Technology. His research interests include wireless communication and big data analysis in the industrial Internet of things. He has authored and coauthored more than 30 refereed international journal and conference papers.



Rongkai Wang (S'18) received the B.Eng. degree in electrical engineering and automation from Hangzhou Dianzi University, Hangzhou, China, in 2016. He is currently working toward the Master's degree in control theory and control engineering at Fuzhou University, Fuzhou, China.

His current research interests include proximity estimation algorithms design, wireless signal processing, and their applications in the mobile industrial human-machine interaction.

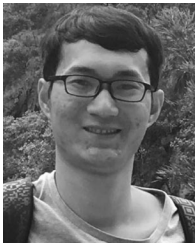
Mr. Wang has authored one paper in the 43rd Annual Conference of the IEEE Industrial Electronics Society (IECON 2017), and one paper in the 1st IEEE International Conference on Industrial Cyber-Physical Systems (ICPS-2018).



Xi Yue received the B.Eng. degree in electrical engineering from Yangtze University of China, JingZhou, China, in 2014 and the Master's degree in control theory and control engineering from Fuzhou University, Fuzhou, China, in 2018.

He is currently a Designer with the Institute of Space Science and Technology, XiaoGan, China. His research interests include the mobile industrial human-machine interaction testbed design and the data analysis based on the testbed.

Mr. Yue has authored one paper in the 43rd Annual Conference of the IEEE Industrial Electronics Society (IECON 2017).



Ting Liu received the B.Eng. degree in automation from the North University of China, Taiyuan, China, in 2014 and the Master's degree in control theory and control engineering from Fuzhou University, Fuzhou, China, in 2017.

He is currently a Software Engineer with Fujian LANDI Commercial Equipment Company, Fuzhou, China. His research interests include proximity estimation algorithms design, wireless signal processing, and their applications in the mobile industrial human-machine interaction.

Mr. Liu has authored one paper in 2017 IEEE International Conference on Communications (ICC 2017).



Cailian Chen (S'03–M'06) received the B.Eng. and M.Eng. degrees in automatic control from Yanshan University, Qinhuangdao, China, in 2000 and 2002, respectively, and the Ph.D. degree in control and systems from the City University of Hong Kong, Hong Kong, in 2006.

In 2008, she was an Associate Professor with the Department of Automation, Shanghai Jiao Tong University, Shanghai, China, where she is currently a Full Professor. Before that, she was a Senior Research Associate with the City University of Hong Kong, Hong Kong, in 2006, and a Postdoctoral Research Associate with the University of Manchester, Manchester, U.K., in 2006–2008. She was a Visiting Professor with the University of Waterloo, Waterloo, ON, Canada, from September 2013 to March 2014. She has worked actively on various topics such as wireless sensor networks and industrial applications, computational intelligence, and distributed situation awareness.

Dr. Chen was honored as the Changjiang Young Scholar by the Ministry of Education of China in 2015 and the Excellent Young Researcher by the National Natural Science Foundation of China in 2016.



Shih-Hau Fang (M'09–SM'13) received the B.S. degree from National Chiao Tung University, Hsinchu, Taiwan, in 1999, and the M.S. and the Ph.D. degrees from National Taiwan University, Taipei, Taiwan, in 2001 and 2009, respectively, all in communication engineering.

He is currently a Full Professor with the Department of Electrical Engineering, Yuan Ze University, Taoyuan City, Taiwan, and is also with the MOST Joint Research Center for AI Technology and All Vista Healthcare, Taiwan. He was a Software Architect with the Chung-Hwa Telecom Company, Ltd., from 2001 to 2007, and was with YZU in 2009. His research interests include indoor positioning, mobile computing, machine learning, and signal processing.

Prof. Fang received the YZU Young Scholar Research Award in 2012 and the Project for Excellent Junior Research Investigators, Ministry of Science and Technology, in 2013. His team won the third place of IEEE BigMM HTC Challenge in 2016, and the third place of IPIN in 2017. He is currently Technical Advisor to HyXen Technology Company, Ltd., and is an Associate Editor for *IEICE Transactions on Information and Systems*.